

AD 742416

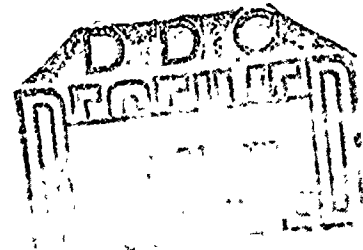
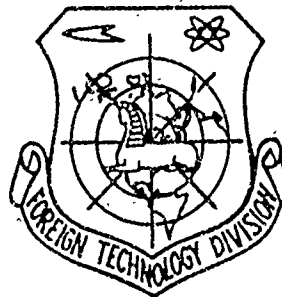
FOREIGN TECHNOLOGY DIVISION
THIS IS AN UNEDITED ROUGH DRAFT TRANSLATION BY
JOINT PUBLICATIONS RESEARCH SERVICES



TRUE STRUCTURE OF MOLYBDENUM AND TUNGSTEN
SINGLE CRYSTALS GROWN FROM THE GAS PHASE

by

W. Reitzenstein, G. Weise



Approved for public release;
Distribution unlimited.

Reproduced by
**NATIONAL TECHNICAL
INFORMATION SERVICE**
Springfield, Va 22151

UNCLASSIFIED

Security Classification

DOCUMENT CONTROL DATA - R & D

(Security classification of title, body of abstract and indexing annotation must be entered when the overall report is classified)

1. ORIGINATING ACTIVITY (Corporate author) Foreign Technology Division Air Force Systems Command U. S. Air Force.		2a. REPORT SECURITY CLASSIFICATION UNCLASSIFIED	
2b. GROUP			
3. REPORT TITLE TRUE STRUCTURE OF MOLYBDENUM AND TUNGSTEN SINGLE CRYSTALS GROWN FROM THE GAS PHASE			
4. DESCRIPTIVE NOTES (Type of report and inclusive dates) Translation			
5. AUTHOR(S) (First name, middle initial, last name) Reitzenstein, W. ; Weise, G.			
6. REPORT DATE 1971		7a. TOTAL NO. OF PAGES 19	7b. NO. OF REFS 13
8a. CONTRACT OR GRANT NO.		9a. ORIGINATOR'S REPORT NUMBER(S) FTD-HC-23-1787-71	
8b. PROJECT NO. 7343		9b. OTHER REPORT NO(S) (Any other numbers that may be assigned this report)	
10. DISTRIBUTION STATEMENT Approved for public release; distribution unlimited.			
11. SUPPLEMENTARY NOTES		12. SPONSORING MILITARY ACTIVITY Foreign Technology Division Wright-Patterson AFB, Ohio	
13. ABSTRACT <p>It is shown that the morphology and crystal perfection of single crystals of Mo and W obtained by vapor deposition using the thermal decomposition of halides, depends on the supersaturation. The crystals were examined by metallographic investigations and X-rays to determine position, extension, and kind of the disturbances. At lower supersaturation, with a given equilibrium form face, disturbances appear regularly in layers and within defined crystallographic positions, which depend on the growth direction in different planes. In most cases the disturbed layer appears in the mirror plane of the planes containing the growth steps. [AP:107866]</p>			

DD FORM 1 NOV 65 1473

UNCLASSIFIED
Security Classification

UNCLASSIFIED

Security Classification

14. KEY WORDS	LINK A		LINK B		LINK C	
	ROLE	WT	ROLE	WT	ROLE	WT
Molybdenum Alloy Tungsten Alloy Metal Single Crystal Metal Vapor Deposition Metallograpny Crystallograpny Refractory Metal X-Ray Technology Thermal Decomposition Chemical Decomposition Halide						

UNCLASSIFIED

Security Classification

UNEDITED ROUGH DRAFT TRANSLATION

by Joint Publications Research Services

TRUE STRUCTURE OF MOLYBDENUM AND TUNGSTEN SINGLE CRYSTALS
GROWN FROM THE GAS PHASE

Author: W. Reitzenstein, G. Weise

English pages: 19

Source: Journal of Crystal Growth 1971, Vol. 9, No. 1,
pp. 228-237

Approved for public release;
distribution unlimited.

GE/0000-71-009-001

THIS TRANSLATION IS A RENDITION OF THE ORIGINAL FOREIGN TEXT WITHOUT ANY ANALYTICAL OR EDITORIAL COMMENT. STATEMENTS OR THEORIES ADVOCATED OR IMPLIED ARE THOSE OF THE SOURCE AND DO NOT NECESSARILY REFLECT THE POSITION OR OPINION OF THE FOREIGN TECHNOLOGY DIVISION.

PREPARED BY:
TRANSLATION DIVISION
FOREIGN TECHNOLOGY DIVISION
WP-AFB, OHIO.

systems⁸ investigated, and with speed of precipitation, if several reactions are neglected which participate in the reaction system. In order to obtain single crystals free of disorders, growth conditions have to be set up which make possible growth by way of two dimensional nucleus formation, or at steps formed by screw dislocations. The load charge and habitus of the equilibrium form planes appearing under these conditions during growth from the gas phase are dependent on the supersaturation. Thus, they determine the macro- and microscopic morphology of the single crystals which, in a certain way, is also predetermined by the rod axis orientation of the support. The morphological findings can be classified as follows:

- 1) Shell or boundary planes which are either
 - a) smooth growing equilibrium form planes and shift parallel in the direction of the normal, or
 - b) coarse planes whose subindividuals are made up from equilibrium form planes
- 2) Surface profiles on the shell planes with crystallographically defined boundaries which are called steps.

There is a close connection between the morphology and the true structure of such crystals in dependence on supersaturation; it can be classified as follows:

1) Growth with little supersaturation on macroscopically and microscopically stepped smooth, and particularly coarsened planes will lead to an inhomogeneous crystal volume. The inhomogeneities characteristic of this growth are designated as disorder areas and layers, and show an extent in the form of sequential dislocation arrangements which is comparable to the build-up of subgrain boundaries up to cracks as coarse disorders in the same crystallographic directions.

2) Growth with higher supersaturation over macroscopically smooth surfaces, especially if all shell planes are equilibrium form planes, will result in a homogeneous (free of disorder areas and layers) crystal volume from molybdenum⁷ made by thermal decomposition homogeneous single crystals with rod axis orientations of $\langle 110 \rangle$, $\langle 100 \rangle$ and $\langle 111 \rangle$ could be obtained which are bound by the equilibrium form planes $\{110\}$, $\{100\}$, $\{211\}$, $\{111\}$ depending on the orientation of the rod axis. Tungsten⁸ grown according

to the same procedure shows {110} exclusively as equilibrium form plane under favorable growth conditions, so that only <111> will lead to exclusive limitation by smooth {110} planes and thus to homogeneous single crystals. It is the goal of this paper to characterize more closely the fine structure of these single crystals with metallographic and x-ray methods. The coarse structure at cracks and sub-grain boundaries can be made visible by optical microscopy where polished {100} planes⁹ also permit proof of dislocations with the help of etch pits, as well as by the Berg-Barrett technique¹⁰; its advantages as against the microscopical procedure were pointed out by Gunther.¹¹ Under the conditions of the particularly clear arrangement of disorder layers built up from dislocation sequences in crystals grown from the gas phase, the Berg-Barrett technique (BB) is at the limit of resolution. The orientation differences of such growth layers were obtained through rocking curves and topographical recordings made with a double-crystal spectrometer (DCS).¹² From the contrast variations of different crystal sections, the DCS method also gives qualitative information on the kind and the preferred type of dislocations in the disorder layers. Of all x-ray topographical procedures the Lang method¹³ offers the most favorable resolution conditions, however, it requires the most expensive sample preparation. The Lang method supplies information on the density, the kind and type of dislocations.

Presently, no theoretical statements are available on the formation of coarse disorders like cracks or even dislocations in crystals grown from the gas phase so that the results on the true structure were only organized according to phenomenology.

2. True Structure of Molybdenum and Tungsten Single Crystals.

2.1 Inhomogeneous Single Crystals.

2.1.1 Interaction of Morphology and True Structure.

To characterize single crystals grown from the gas phase over macroscopically stepped shell planes, the designations growth region, - layer and disorder region layer will be used. Growth regions are the crystal volumes grown

radiarily into the various crystallographic directions which are bound at the surface by shell planes. The growth layers are positioned in the growth regions and are the crystal volumes which are bound at the surface by the profile of the steps on the shell planes. Disorder regions are the transition regions between growth regions and disorder layers are the boundary planes of growth layers.

Fig. 1 shows a schematic of the growth and disorder orientations for a $\langle 110 \rangle$ single crystal. Growth areas extend into $\langle 211 \rangle$ and $\langle 110 \rangle$ directions, also, $\langle 100 \rangle$ and $\langle 111 \rangle$ regions may occur depending on the growth conditions. The disorder regions and disorder layers appear at the following places in the order of their extent:

- a) disorder regions between colliding growth regions,
- b) disorder layers as a trace of the hollow edges of steps on coarsened planes,
- c) disorder layers as trace of the hollow edges on smooth planes.

Furthermore, the extent of these disorders decreases with increasing supersaturation. This is caused by a reduced supersaturation in the border region of the shell plane and in the hollow edges of the steps. This shows up as a sensitive characteristic of supersaturation at the morphological appearances of the step formation. This supersaturation gradient towards the border region of the macroscopic shell planes, as represented schematically in Fig. 2, is larger than in the profile of the steps of convex and enclosed edge (Fig. 2). Thus, from the standpoint of the supersaturation gradient the extent of the disorders is larger in the disorder regions than in the disorder layers. The flatter the surface relief of the steps is developed on the shell planes the smaller is the supersaturation gradient and with it the degree of disorder.

A few examples will demonstrate the dependence on supersaturation of these disorders. Low supersaturations with macro steps on the shell planes (Fig. 3) lead to cracks in the disorder regions and layers (Fig. 3b). Due to bigger subindividuals the disorder region between the $\langle 211 \rangle$ growth regions shows more pronounced cracks than that between $\langle 211 \rangle$ - $\langle 110 \rangle$.

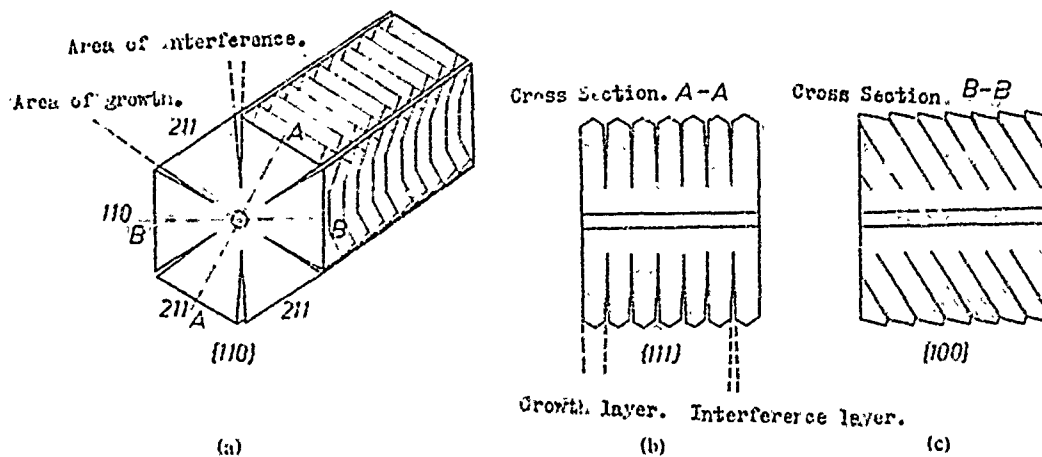


Fig. 1. Schematic representation of the growth and disorder regions as well as growth and disorder layers for a $\langle 110 \rangle$ single crystal. a) disorder regions between colliding 211 and $\langle 110 \rangle$ growth regions. Depending on the degree of supersaturation between the $\langle 211 \rangle$ regions there will also be a $\langle 100 \rangle$ growth region. b) Disorder layers as trace of the hollow edges of steps on coarse planes. c) Disorder layers as trace of the hollow edges on smooth planes.

The crack shaped disorder layers in the growth regions clearly can be associated with the traces of the hollow edges of the steps. The interval of the steps on the surface correlates with the distances of the cracks in the crystal volume. Relatively higher supersaturations lead to more steps on the shell planes and to disorder layers in the growth regions which exhibit dislocation sequence in the typical arrangement of the subgrain boundaries as is shown by the (010) polished cross sections of a $\langle 110 \rangle$ tungsten single crystal.

The expansion of the disorders to a three dimensional

crack can be seen clearly in the $\{100\}$ growth region in Fig. 4. It is caused by larger subindividuals with increasing layer thickness. The possibility in principle of a disorder free growth is pointed out by the undisturbed initial layer. The crystallographic location and the build-up of the disorder layers which are well visible on the higher light optical micrographs of Fig. 4b are discussed taking the $\langle 110 \rangle$ tungsten single crystal shown in Fig. 4 as an example.

2.1.2 Crystallographic location and build-up of the disorder layers.

Since only plane orientations around (100) can be etched metallographically an investigation of several crystal sections was carried out through combination with the x-ray DCS method. The goal was to determine the crystallographic position of the disorder layers caused by the surface profile and the degree of reciprocal angles of the growth layers which for larger orientation differences can be seen in the splitting of Laue reflexes.

The following results were obtained:

a) The mirror symmetry plane or the bisecting line of the angle of the planes of the growth steps on the shell planes result as the crystallographic location of the disorder layers between the growth layers. Thus, the following disorder layers (Fig. 5) appear for single crystals with $\langle 110 \rangle$ rod axis orientation in the growth regions of the corresponding shell planes.

Shell planes $\{110\}$:

Growth region	$(\bar{1}10)$:	
Growth steps:	$(\bar{1}10), (011)$:	disorder layer: (101) :
Growth steps:	$(\bar{1}10), (01\bar{1})$:	disorder layer: $(10\bar{1})$.

Growth region	$(1\bar{1}0)$:	
Growth steps:	$(1\bar{1}0), (0\bar{1}1)$:	disorder layer: (101) :
Growth steps:	$(1\bar{1}0), (0\bar{1}\bar{1})$:	disorder layer: $(\bar{1}01)$.

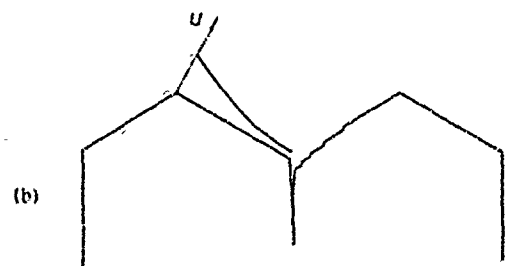
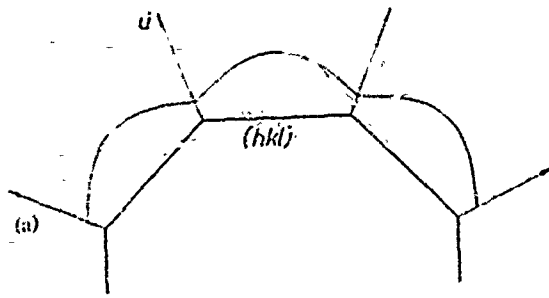


Fig. 2. Schematic representation of the supersaturation gradient above the snell planes (a) and above the macro steps (b).

In the metallographic (101) section (Fig. 4b) these disorder layers run obliquely in $\langle 110 \rangle$ directions, in the (100) section horizontally in the direction $\langle 100 \rangle$.

If the crystallographic axis is identical with the z axis then on each $\{110\}$ snell plane all four $\{110\}$ growth steps will appear which lead to a total of four effective $\{110\}$ disorder layers.

Shell planes $\{211\}$:

Growth steps: $\{110\}$ with the zone axes $[1\bar{1}1]$
 (111) ;
 Disorder layers: (110) .

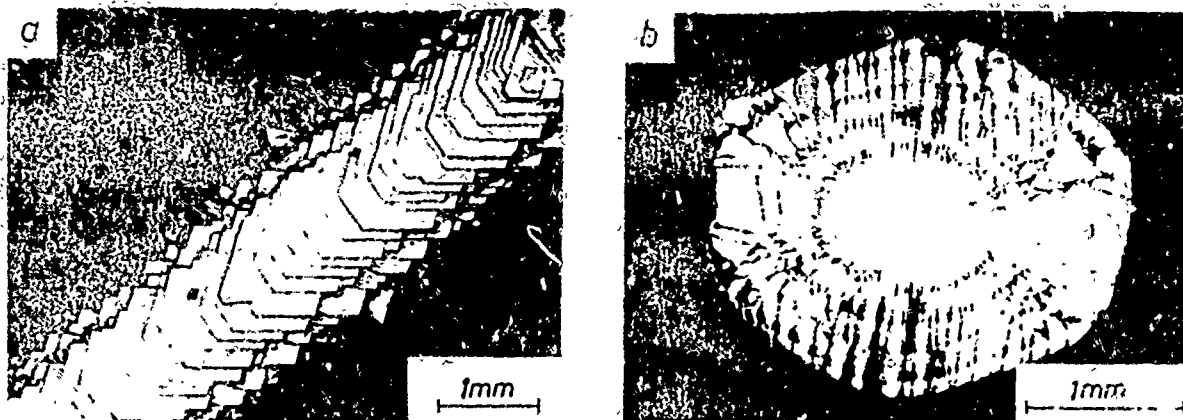


Fig. 3. $\langle 110 \rangle$ Molybdenum single crystals with low supersaturation: (a) $\{110\}$ shell plane with $\{110\}$ macro steps. (b) Crack snapped disorder regions and layers in the crystal volume.

In the metallographic (010) cut (Fig. 4a,c) the disorder layer is perpendicular in the direction $\{001\}$.

Shell planes $\{100\}$:

Growth steps: (011), (101), (0 $\bar{1}$ 1), ($\bar{1}$ 01);

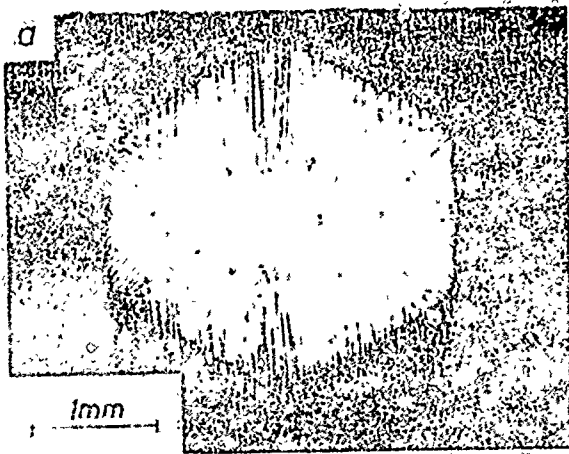
Disorder layer: $\{110\}$ with zone axis $[001]$;

Disorder layer: $\{100\}$ with zone axis $[001]$.

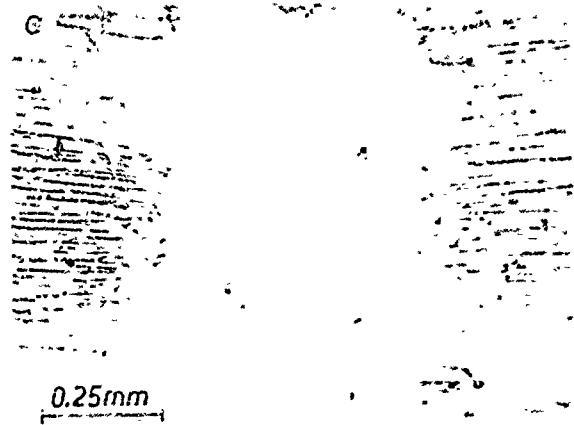
In the metallographic (010) section (Fig. 4a) the disorder layers are parallel to (001). Fig. 6 shows the various locations in the (001) section.

The extent of the disorders in the crystals depends on the height difference in the surface relief. The degree of disorder continues to be the result of the number of effective disorder layers. This number is highest in the $\{100\}$ shell plane region so that this region is disturbed the most. In the disorder region $\{110\}$ - $\{211\}$ the disorder layers of the neighboring growth regions (Fig. 3b) penetrate each other and lower supersaturations lead to the formation of cracks.

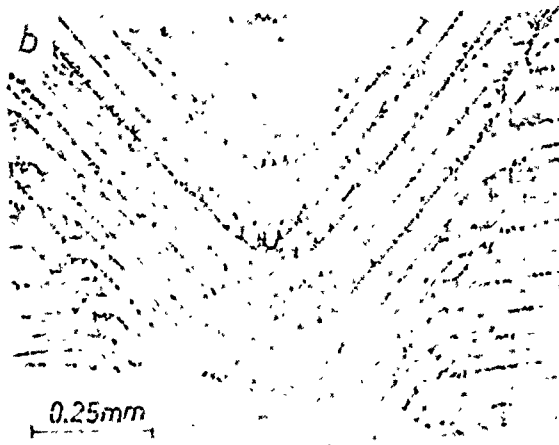
(b) In order to determine the kind and type of dislocation



4(a)



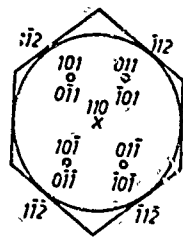
4(b)



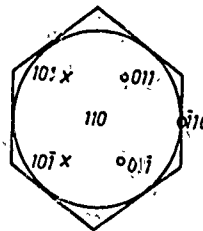
4(c)

Reproduced from
best available copy.

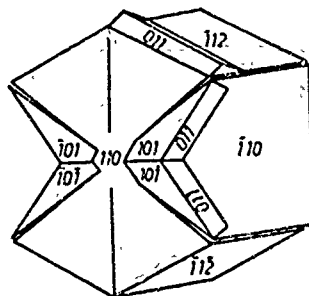
Fig. 4: Subgrain boundaries as disorder layers in a (010) polished cross section of a Cu single crystal. (a) Survey photograph, 25x. (b) Position of the subgrain boundaries in the Cu region, 100x. (c) Position of the subgrain boundaries in the Cu and Zn region, 100x.



(211) shell planes
 o growth steps
 x disorder layer



(110) shell planes
 o growth steps
 x disorder layer



arrangement of the disorder
 layers in the region of the
 (110) - shell planes

Fig. 5: Schematic representation of the location of the disorder layers in (110) single crystals.

In the disorder layers the orientation and extinction x-ray contrast on (001) , $(1\bar{1}2)$, $(1\bar{1}\bar{1})$ and (110) sections were compared. The experimental findings showed that the $\{110\}$ disorder layers between growth layers are built up from dislocations with a predominant share of steps. Qualitatively, the contrasts can be associated with dislocations of the type $b = 1/2 [1\bar{1}\bar{1}]$ and $b = 1/2 [1\bar{1}\bar{1}]$ (Fig. 7).

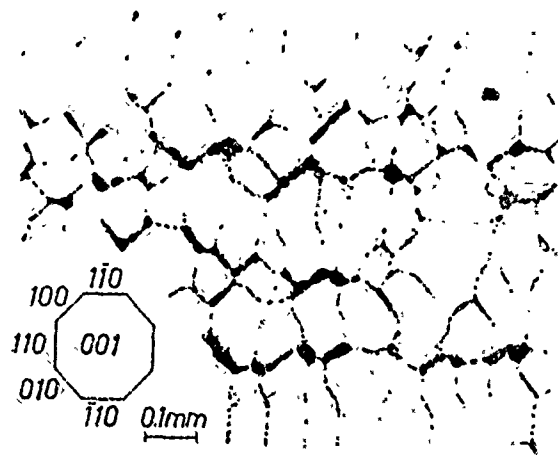


Fig. 6: (001) layer with (110) and (100) disorder layers in the (001) growth region.

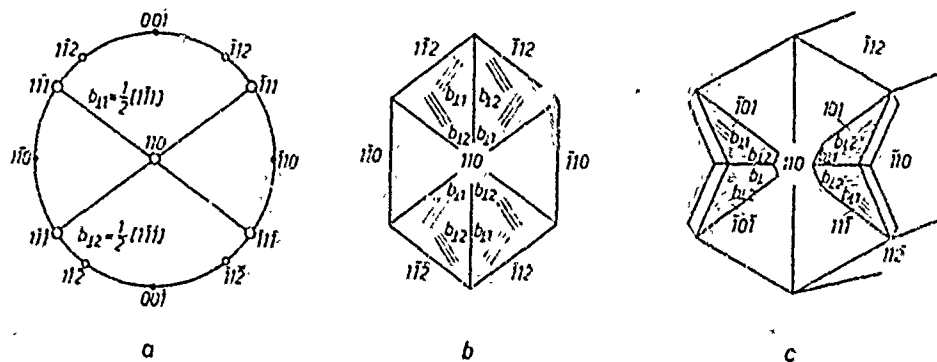


Fig. 7: Location of the possible step dislocations in the disorder layer. (a) Representation in stereographic projection, (b) in the (110) disorder layer of the (001) growth regions, (c) in the (110) disorder layers of the (110) growth regions.

The (100) disorder layers appearing in the (001) growth region ought to be built up from step dislocations only.

(c) From the distance of the rows of etch figures the width of the growth layers turns out to be about $50\mu\text{m}$. This corresponds to the distances of the fine-stripes on the x-ray films (Fig. 3a) which, therefore, can be associated with the

growth layers.

(d) From the distance of the etch figures in the disorder layers $D \leq 5 \mu\text{m}$ the reciprocal angles between the growth layers is $\theta \leq 0.2$ angle minutes with the simplified assumption of $\theta = b/D$. In agreement with this it was found that the orientation differences determined with x-rays are of the order of magnitude of 1 angle minute. It can be seen from the rocking curves of large crystal regions with about 100 growth layers that these reciprocal angles do not add up in the same sense of rotation to a correspondingly high orientation width but obviously occur with alternating direction of rotation. This can be explained with a change of the sign (+, -) of the dislocations in the neighboring disorder layers.

(e) The substrates for the manufacture of single crystals, made through recrystallization after critical deformation, have a subgrain structure which continues in the material growing on them in the form of "growth regions" of different orientation. These growth regions (designated B) are causing the coarse picture structuring in Fig. 8 with reciprocal angles of several minutes. Based on the appearance of contrast at various oriented sections it is assumed that the disordered transition layers between the growth regions consist mainly of screw dislocations with $b = 1/2 [111]$.

(f) The DCS picture of the $(\bar{1}10)$ shell plane (Fig. 9) shows a cell structure within the growth layers. It results from the combined appearance of (011) , $(\bar{0}11)$ growth steps and with this, also growth layers of (101) and $(\bar{1}01)$. The partial pictures (recorded with one minute difference each in the angle of incidence make clear the reciprocal angles between the cells which is due to an accumulation of predominantly step dislocations.

2.2 Homogeneous single crystals.

A homogeneous crystal volume is formed by growth over macroscopically smooth shell planes as is shown in Fig. 10 for a $\langle 100 \rangle$ molybdenum single crystal with four each $\{110\}$ and $\{100\}$ shell planes. The following can be said about the true structure:

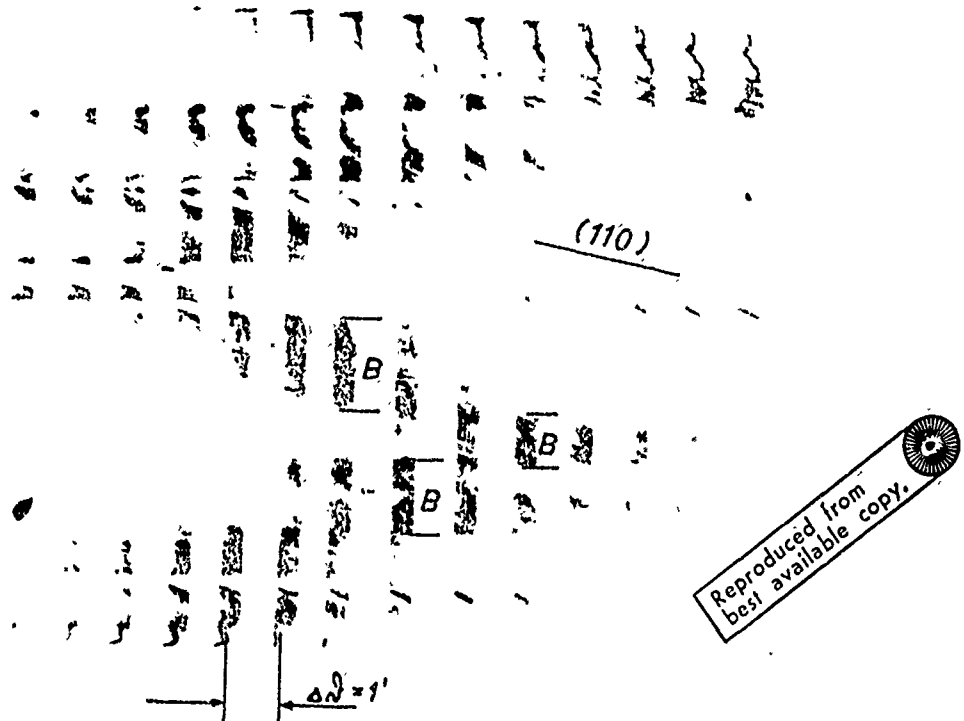


Fig. 8: DCS picture of an inhomogeneous tungsten single crystal. (111) section through (20) growth regions. The stripe-shaped partial pictures are obtained by stepwise change of the angle of incidence. The fine-stripes can be attributed to the growth layers or (110) disorder layers, respectively and the coarse picture structuring to the growth regions.

(a) No phase boundary can be noticed between the substrate and the layer grown on it. The regions only differ by density of dislocations.

(b) In the layer grown on the substrate subgrain boundaries may be present. The causes for this could be:

[1] accidental supersaturation inhomogeneities in the growth conditions;

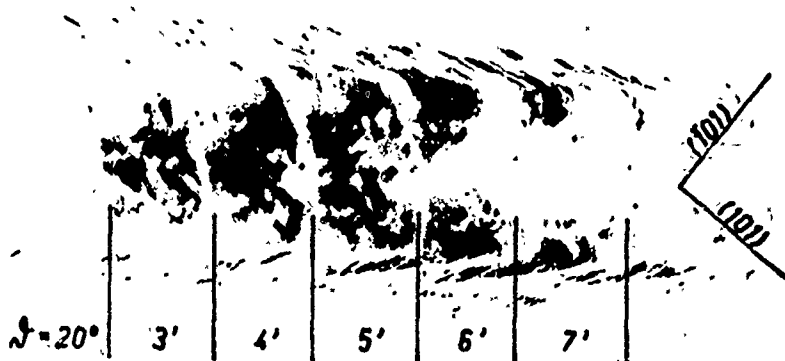


Fig. 9: DCS picture of the $(\bar{1}10)$ shell plane of an inhomogeneous tungsten single crystal. The cell structure is formed by (101) and $(\bar{1}01)$ disorder layers intersecting each other.

[2] impurities on the surface of the substrate;

[3] subgrain boundaries present in the substrate continue into the layer growing on it as can be shown metallographically, and on BB pictures (Fig. 11a,b). Zone molten rods used as substrates always exhibit such subgrain boundaries while single crystalline filaments made through recrystallization after critical deformation largely are free of these disorders (Fig. 11c).

(c) The layer deposited from the gas phase shows low disorder densities which have been caused by the following methodic advantages:

[1] small temperature gradient, and, thus, avoidance of thermal stresses:

[2] high thermal purity of the halides as base material this includes decreased solubility of the components of the remaining gas atmosphere;

[3] low void concentration with low deposition temperatures.

The pictures of the sections were enlarged with an optical microscope, they have low resolution and show an

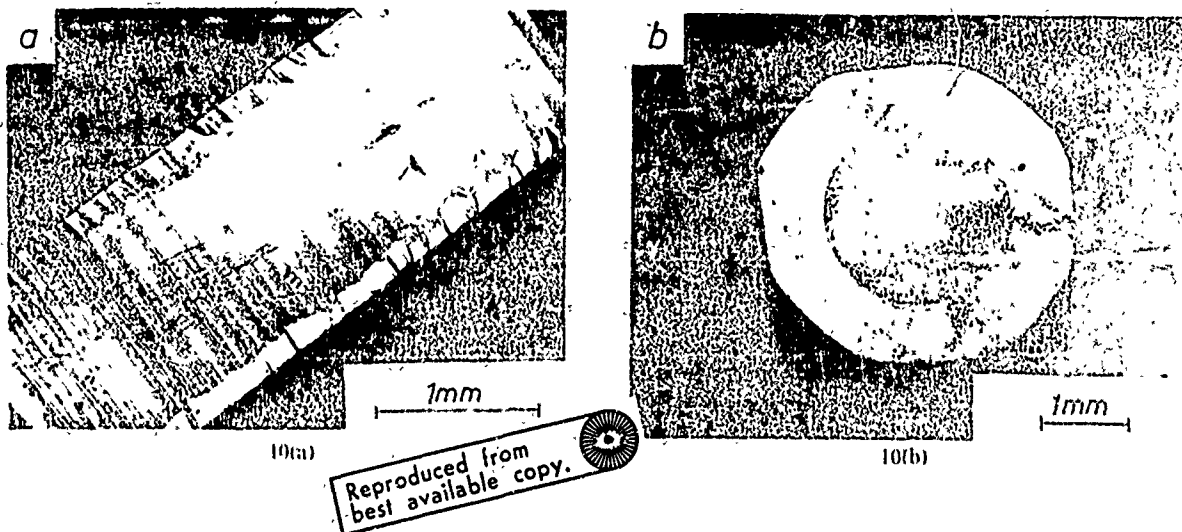


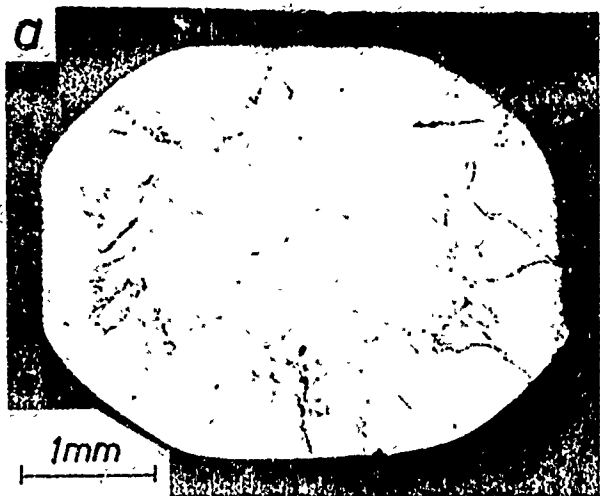
Fig. 10: $\langle 100 \rangle$ molybdenum single crystal with high supersaturation: (a) macroscopically smooth surface, (b) homogeneous crystal volume.

irregular distribution of the dislocations. The Lang technique, however, provides data on the density, kind and type of the dislocations. Topographies of various $\{110\}$ reflexes were made of a $\langle 100 \rangle$ molybdenum single crystal free of subgrain boundaries. The pictures (Fig. 12) yield the following results:

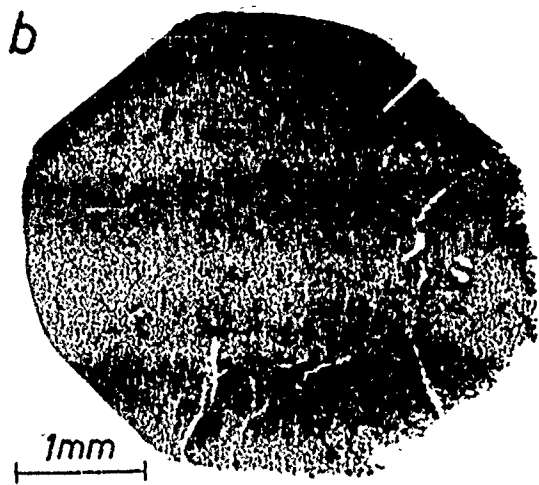
(a) in the growth regions of the shell planes of $\{110\}$ and $\{100\}$ the crystal shows contrasts from dislocation groups and single dislocations. Contrast appearances due to anomalous transmission point can lead to a dislocation density of 10^4 cm/cm^2 .

(b) Geometry of the dislocation arrangement, the contrasts and the possible Burgers vectors point to step dislocations of the type $b = 1/2 \langle 111 \rangle$.

(c) The contrasts in the $\{110\}$ and $\{100\}$ growth regions are positioned parallel to $\langle 110 \rangle$ directions. These dislocations shown in the picture with $b = 1/2 \langle 111 \rangle$ and $\sigma = \langle 211 \rangle$ along the planes possible with $\langle 211 \rangle$ as zone axis are probably located in $\{110\}$ planes, analogous to the importance of $\{100\}$ as growth and disorder planes for the

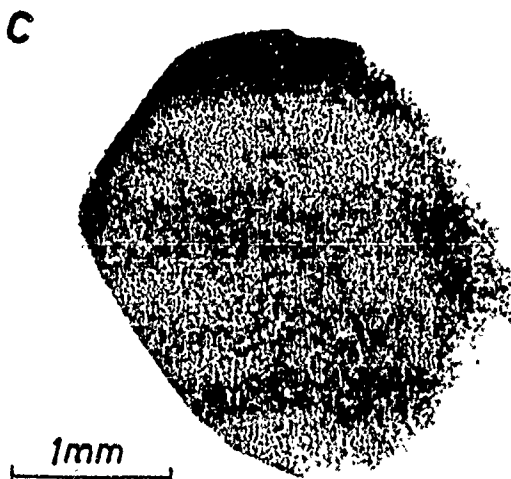


11(a)



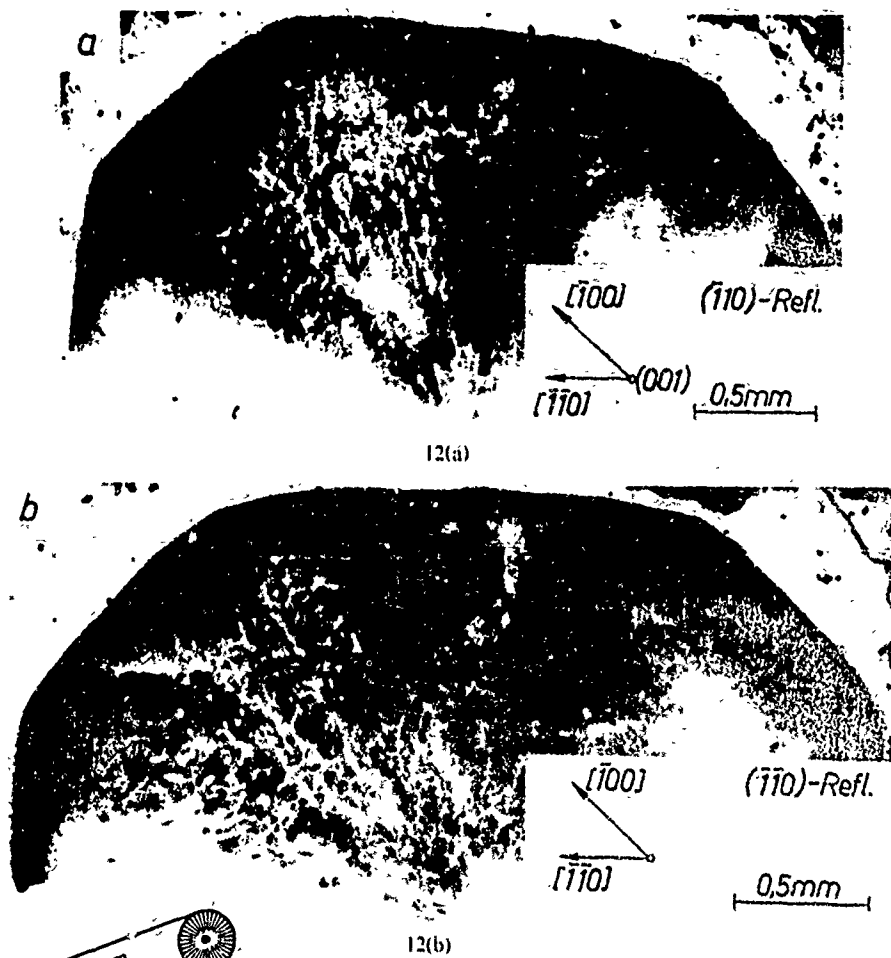
11(b)

Reproduced from
best available copy.



11(c)

Fig. 11: Influence of the true structure of the substrate on the layer growing on it. (a) $\{100\}$ cross-section of a $\langle 110 \rangle$ molybdenum single crystal with subgrain boundaries from the zone molten substrate. (b) proof of such subgrain boundaries with BB pictures. (c) BB picture of a single crystal free of subgrain boundaries with single crystalline substrate made through recrystallization.



Reproduced from
best available copy.

Fig. 12: Lang pictures of dislocation structures in the (001) section of a molybdenum single crystal: (a) topography with $(\bar{1}10)$ reflex; (b) topography with $(\bar{1}10)$ reflex.

inhomogeneous crystals. In the $\{100\}$ growth region a preferred direction of the contrasts towards $\langle 310 \rangle$ to $\langle 210 \rangle$ can be found. These dislocations are built up from partial pieces with step character which also ought to be located in $\{110\}$ planes.

3. Summary

The morphology of single crystals grown from the gas phase is a result of the combination of equilibrium form planes. Low supersaturations lead over stepped, microscopically smooth planes, and especially coarsened planes, to an inhomogeneous crystal volume. With higher supersaturations growth takes place over macroscopically smooth planes and results in homogeneous single crystals with a low dislocation density ($<10^4 \text{ cm}^{-2}$) free of disorder regions and layers. Disorders in the inhomogeneous crystals are arranged in layers whose crystallographic location is determined by morphology. It was found that the disorder layer is always the plane of mirror symmetry of the planes of neighboring growth steps. Therefore, the preferential position of the $\{110\}$ equilibrium form plane and the $\{110\}$ steps on smooth and coarsened shell planes resulting from it, lead predominantly to $\{110\}$ disorder layers. The disorder layers contain mainly dislocations with step character of the type $b = 1/2 \langle 111 \rangle$ which cause alternating tilting in the order of magnitude of one angle minute between neighboring growth layers. Larger orientation differences in the single crystals are due to disorders in the substrate which continue into the volume growing on it.

We would like to thank Dr. P. Finke for the metallographic investigations, also Dr. C. Becker for providing and discussing the Lang-topographies, and Dr. H. Wadewitz for the investigations with the Berg-Barrett technique.

BIBLIOGRAPHY

1. A. E. Van Arkel, Reine Metalle, Springer, Berlin, 1939
2. H. Schaefer, Chemische Transportreaktionen (Chemical Transport Reactions), Verlag Chemie Weinheim, 1962
3. I. N. Stranski and R. Kaischew, Z. Physik. Chem. Vol B26, pp 100, 114, 312, 1934.
4. F. C. Frank, in "Growth and Perfection of Crystals", Ed. R. H. Doremus et al, Wiley, New York, 1958, p 441.
5. A. A. Tschernov, Kristallografiya (Crystallography), Vol 7, p 895, 1962; Vol 8 p 87, 1963.
6. G. Weise, Kristall und Technik, Vol 2, No. 3, p 339, 1967.
7. G. Weise and R. Guenther, J. Crystal Growth, Vol 6, p 167, 1969-1970

8. G. Weise and R. Owsian, J. Less-Common Metal, Vol 20, p 99, 1970
9. P. Finke, Prakt. Metallog. Vol 2, No 4, p 151, 1965
- 10 H. Wadewitz, Reinststoffprobleme in Wessenschaft und Technik, Vol 3, Ed. E. Rexer, Akademie-Verlag, Berlin, 1967, p 301
11. F. Guenther, Freiburger Forschungsh., Vol B141, Metallkunde 1969, p 161.
12. W. Reitzenstein, Dissertation, DAW, Berlin, 1971
13. C. Becker, Dissertation, DAW, Berlin, 1970

- END -